

PAPER

RIS-Assisted MIMO OFDM Dual-Function Radar-Communication Based on Mutual Information Optimization

Nihad A. A. ELHAG[†], Liang LIU^{†a)}, Ping WEI[†], *Nonmembers*, Hongshu LIAO[†], *Member*, and Lin GAO[†], *Nonmember*

SUMMARY The concept of dual function radar-communication (DFRC) provides solution to the problem of spectrum scarcity. This paper examines a multiple-input multiple-output (MIMO) DFRC system with the assistance of a reconfigurable intelligent surface (RIS). The system is capable of sensing multiple spatial directions while serving multiple users via orthogonal frequency division multiplexing (OFDM). The objective of this study is to design the radiated waveforms and receive filters utilized by both the radar and users. The mutual information (MI) is used as an objective function, on average transmit power, for multiple targets while adhering to constraints on power leakage in specific directions and maintaining each user's error rate. To address this problem, we propose an optimal solution based on a computational genetic algorithm (GA) using bisection method. The performance of the solution is demonstrated by numerical examples and it is shown that, our proposed algorithm can achieve optimum MI and the use of RIS with the MIMO DFRC system improving the system performance.

key words: *dual-functional radar-communication (DFRC), multiple-input multiple-output (MIMO), reconfigurable intelligent surface (RIS), orthogonal frequency division multiplexing (OFDM), genetic algorithm (GA)*

1. Introduction

Contemporary wireless communication systems are rapidly evolving, driven by a growing demand for enhanced capacity, accelerated data rates, and efficient utilization of the radio spectrum [1]–[3]. Dual-Function Radar-Communication (DFRC) strategies emphasize the design of the integrated systems capable of executing simultaneous wireless communication and remote sensing tasks and found applications in many areas [4], [5]. The features of the DFRC system include compact system size, augmented operational efficiency, and decreased power consumption and improved spectral effectiveness [4], [6]–[9].

A significant challenge faced by DFRC systems is the complex task of waveform design, which has progressively emerged as a crucial domain warranting academic investigation. The OFDM technique is suitably equipped for radar and communication tasks as it offers efficient system implementation and high spectrum efficiency [6], [10], [11].

DFRC systems, in practical applications, may experience signal degradation due to obstacles or structures

obstructing the signal path. This has encouraged an exploration into utilizing Reconfigurable Intelligent Surfaces (RIS) within DFRC systems [12]. The primary attraction of RIS lies in its ability to significantly boost both spectrum and energy efficiency. Fundamentally, a RIS is a planar array filled with passive reflectors. Each unit can independently adjust the phase of incoming signals and reflect it towards the intended destinations [12]–[19].

The primary challenge is the development of methods that optimize system performance without transgressing set constraints. Our research delves into the formulation of a joint OFDM waveform, encompassing considerations for both radar and user receive filters design, within the context of a RIS-Assisted MIMO DFRC system.

Numerous studies have probed into the integration of radar and communication systems, outlining different approaches to amplify system performance, including joint resource management [6], [20]–[23].

Radiated waveforms and the radar and user receive filters of the MIMO DFRC system were developed in communication-centric system. Such method optimize radar-driven objectives that take into account parameters such as average transmission power, direction-specific power leakage, and individual user error rates, while maintaining communication quality of service (QoS). The design process integrates both the estimation and detection-driven merit functions into a design framework. These method use alternating optimization, the establishment of a convex boundary for possible search, and the employment of minorization-maximization techniques. However the method does not guarantee convergence to a local or global optimal solution [24].

The beamforming problem in a RIS aided DFRC system requires the solution of a set of non-convex equations. These could be solved by relaxation methods, Riemannian conjugate gradient methods and penalty-based techniques. Again, the methods are based on approximating the objective functions to convert the problem into a convex problem [25]. Also, the non-convex problem for the resource allocation in a MIMO DFRC system can be converted into two convex sub-problems [22].

A joint design of transmit beamforming and RIS reflecting for radar sensing and single-user communications has been demonstrated [26]. On the other hand, a passive beamformer design in a RIS-Aided DFRC system was designed to meet the communication requirements of the users

Manuscript received November 2, 2023.

Manuscript revised January 31, 2024.

Manuscript publicized March 15, 2024.

[†]School of Information and Communication Engineering, University of Electronic Science and Technology of China, Chengdu 611731, Sichuan, China.

a) E-mail: liu_yinliang@outlook.com (Corresponding author)

DOI: 10.1587/transfun.2023EAP1138

[25]. The RIS has also been used to enhance the energy efficiency of the DFRC system [27]. Furthermore, the RIS can be used to relay signals in the uplink and downlink directions [25]–[27].

From the aforementioned studies, it is clear that mutual information (MI) metric has not been considered for joint OFDM waveform design together with radar and user receive filters' design of MIMO DFRC system. Therefore, this motivates us to investigate MI in such systems. Moreover, existing research appears to neglect scenarios where a target or user is located in a blind spot. This paper considers this issue, while optimizing a radar-oriented objective function and simultaneously ensuring efficient user communication.

In contrast with preceding studies, and motivated by the significant advantages of RIS, the main contribution of this paper can be summarized as follows:

- We explore a joint OFDM waveform design of a MIMO OFDM DFRC system with RIS assistance. RIS is utilized to reach blind spots and create indirect paths together with Line-of-Sight (LoS) paths.
- We demonstrate that the proposed joint OFDM waveform, radar and user receive filters' design, is conceived as a comprehensive resource allocation problem. The radar performance is optimized via MI, while complying with constraints on average transmit power, the transmit beampattern, and individual user error rates.
- Our methodology incorporates the scenario where the radar concurrently handles multiple targets on the same subcarrier.
- An optimal solution for the inherently non-convex optimization problem is presented through the application of the Genetic Algorithm (GA) using bisection method. The performance of the proposed solution is showcased through a series of numerical examples and simulations.

Section 2 of this paper introduces the system model. In Sect. 3, the optimization problem is formulated, while an efficient algorithm is proposed to address the formulated optimization problem in Sect. 4. Section 5 presents numerical results to evaluate the performance of the proposed designs. Finally, Sect. 6 concludes the paper.

In this paper, matrices and vectors are denoted by bold uppercase letters (i.e., \mathbf{X}) and bold lowercase letters (i.e., \mathbf{x}), respectively. \mathbb{C} is the set of complex number, j indicates the imaginary unit and \mathbf{I}_N is the $N \times N$ Identity matrix. The superscripts $(\cdot)^*$, $(\cdot)^T$ and $(\cdot)^H$ indicate conjugate, transpose and conjugate transpose, respectively. $\text{Tr}(\mathbf{X})$ is the trace of a square matrix \mathbf{X} , $\text{vec}(\mathbf{X})$ is the vector obtained by stacking up the columns of \mathbf{X} and $\text{diag}(\mathbf{x})$ is the diagonal operation. \otimes indicates the Kronecker product.

2. The System Model

This section describes a MIMO OFDM DFRC system with RIS composed of L elements, as shown in Fig. 1. The system consists of a DFRC transmitter, a co-located radar receiver, and M communication users, each equipped with a linear

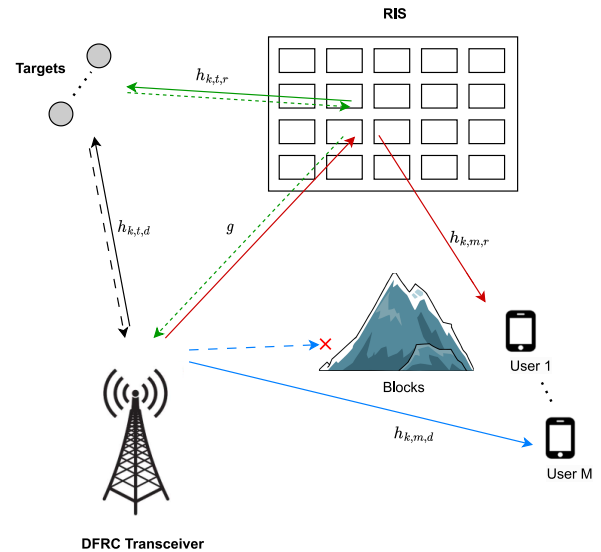


Fig. 1 RIS-assisted MIMO dual-function radar-communication.

array with closely spaced antennas. The number of antennas at the transmitter, the radar receiver, and the m -th user are represented as N_t , N_r , and N_m , respectively. Given that the duration of an OFDM symbol is longer than the propagation delay, narrowband assumptions hold on each subcarrier k . On each shared subcarrier k , the transmitter will broadcast a message while illuminating the direction of a prospective target.

The RIS could be viewed as a reflector with an angle of incidence, θ_i , and an angle of reflection θ_r . The RIS has the additional property to control the phase of the reflected signal, while incurring no loss [16], [28].

The total path loss between a source and a destination via an RIS should also be correctly modelled. This is an area of active research and various models have been proposed, [29]–[32]. Experimental measurements to validate the models have been reported, e.g. [30]. The model in [29] and [30] take the physical geometry and spatial orientation of the RIS into account. Assuming that the distance between the source and the RIS is ds_1 and the distance between the RIS and the destination is ds_2 , reference [31] proposes a reflection model that shows the power loss at the destination is inversely proportional to the sum of the two distances as follows:

$$PL \propto (ds_1 + ds_2)^{-2}. \quad (1)$$

On the other hand, scattering models in electrically small RIS using isotropic models assume that the RIS retransmits the signal in all directions. This scattering model effectively expresses the overall path loss as the product of two losses, resulting in a total path loss of [31]:

$$PL \propto (ds_1 ds_2)^{-2}. \quad (2)$$

The experimental results have shown that the path loss in the far field region could be approximated better by (1) and this model is adopted in this study.

2.1 Radar Model

The radar inspects the direction φ_k on subcarrier k and it is aware of the presence of the self-interference (clutter) which is caused by $C \geq 0$ independent scatterers located in the directions $\vartheta_c \cdots \vartheta_C$ where $\vartheta_c \neq \varphi_k$ for any c and k . As RIS panel is deployed, each target is able to receive both reflected signal from the RIS and LoS signal from DFRC transmitter. Hence, the discrete-time signal received on the k -th subcarrier can be modeled as follows [24] [12]:

$$\begin{aligned} r_k = & \mu_k \left(h_{k,t,d} \text{Tr} \left(\mathbf{W}_k^H \mathbf{b}_k(\varphi_k) \mathbf{a}_k^T(\varphi_k) \mathbf{U}_k \right) \right. \\ & + \left. \left(\mathbf{h}_{k,t,r}^H \mathbf{\Phi} \mathbf{g} \right) \text{Tr} \left(\mathbf{W}_k^H \mathbf{b}_k(\varphi_k^{RIS}) \mathbf{a}_k^T(\varphi_k^{RIS}) \mathbf{U}_k \right) \right) \text{(Target)} \\ & + \mu_k \sum_{c=1}^C \eta_{k,c} \text{Tr} \left(\mathbf{W}_k^H \mathbf{b}_k(\vartheta_c) \mathbf{a}_k^T(\vartheta_c) \mathbf{U}_k \right) \text{(Clutter)} \\ & + \text{Tr} \left(\mathbf{W}_k^H \mathbf{Z}_k \right), \end{aligned} \quad (3)$$

where: $h_{k,t,d} \in \mathbb{C}$ is the response of the direct path from transmitter to the target, $\mathbf{h}_{k,t,r} \in \mathbb{C}^L$ is the response of the path from RIS elements to the target and $\mathbf{g} \in \mathbb{C}^L$ is the response of the path from transmitter to RIS elements. $\mathbf{\Phi} \triangleq \text{diag}(\boldsymbol{\phi}^H)$, $\boldsymbol{\phi} \in \mathbb{C}^L$ is the phase shift vector of the RIS, $\boldsymbol{\phi} = [e^{j\theta_1}, \dots, e^{j\theta_L}]^H$, where $\theta_l \in [0, 2\pi)$. $\varphi_k, \varphi_k^{RIS}$ are the corresponding angles of arrival and departure for the target through the direct path and RIS path, respectively, while (ϑ_k) is the corresponding angles of arrival and departure for the clutter; $\mathbf{b}_k(\varphi) \in \mathbb{C}^{N_r}$ and $\mathbf{a}_k(\varphi) \in \mathbb{C}^{N_t}$ are the receive and transmit steering vectors, respectively, which are normalized to have entries with unit magnitude; for example, if a uniform receive array is employed, we have $\mathbf{b}_k(\varphi) = [1, e^{-j2\pi \frac{\nu_k \ell}{c} \sin(\varphi)}, \dots, e^{-j2\pi \frac{\nu_k \ell}{c} \sin(\varphi)(N_r-1)}]^T$ where ν_k is the center frequency of the k -th subcarrier, ℓ is the element spacing, and c is the speed of light; $\mathbf{U}_k \in \mathbb{C}^{N_r \times T}$ is the code matrix employed by the transmitter, which spans T OFDM symbols and $\mathbf{W}_k \in \mathbb{C}^{N_r \times T}$ is the filter employed radar receiver; $\mu_k \in M\mathcal{D} = \{1, e^{\frac{j2\pi}{MD}}, \dots, e^{\frac{j2\pi(MD-1)}{MD}}\}$ is the Differential Phase Shift Keying (DPSK) symbol to be broadcast, with MD being the cardinality of the constellation $M\mathcal{D}$; $\mathbf{Z}_k \in \mathbb{C}^{N_r \times T}$ is the disturbance vector.

By taking $\mathbf{u}_k = \text{vec}(\mathbf{U}_k)$, $\mathbf{w}_k = \text{vec}(\mathbf{W}_k)$, $\mathbf{z}_k = \text{vec}(\mathbf{Z}_k)$ and $\mathbf{B}_k(\vartheta_c) = \mathbf{I}_T \otimes \mathbf{b}_k(\vartheta_c) \mathbf{a}_k^T(\vartheta_c)$, so, the received signal can be rewritten as follows:

$$\begin{aligned} r_k = & h_{k,t,d} \mathbf{w}_k^H \mathbf{B}_k(\varphi_k) \mathbf{u}_k + \left(\mathbf{h}_{k,t,r}^H \mathbf{\Phi} \mathbf{g} \right) \mathbf{w}_k^H \mathbf{B}_k(\varphi_k^{RIS}) \mathbf{u}_k \\ & + \sum_{c=1}^C \eta_{k,c} \mathbf{w}_k^H \mathbf{B}_k(\vartheta_c) \mathbf{u}_k + \mathbf{w}_k^H \mathbf{z}_k, \end{aligned} \quad (4)$$

and the corresponding signal-to-interference-plus-noise ratio (SINR) can be rewritten as (5).

When the radar simultaneously inspects multiple directions on the same subcarrier, it can handle multiple targets on the same subcarrier. The corresponding SINR can be written as (6), where N is the number of targets. Therefore, the conditioned mutual information (MI) can be written as follows:

$$\text{MI}_k = \log(1 + \text{SINR}_k), \quad (7)$$

$k = 1, 2, \dots, K$.

The SINR represents the power ratio between the desired signal and the interference-plus-noise, while the conditioned mutual information (MI) represents the information content and the reduction in uncertainty about the transmitted radar signal after conditioning on interference and noise.

2.2 Communication Model

Desired and/or undesired ($J_m \geq 0$ which are caused by as many far-field independent scatterers) paths can be present between the transmitter and the m -th user. Each m -th user can receive both reflected signal and LoS signal from the DFRC transmitter as the RIS panel is deployed. Hence, its discrete-time received signal on the k -th subcarrier can be modeled as follows:

$$\begin{aligned} r_{k,m} = & \mu_k \left(h_{k,m,d} \text{Tr} \left(\mathbf{W}_{k,m}^H \mathbf{b}_{k,m}(\bar{\omega}_{m,0}) \mathbf{a}_k^T(\omega_{m,0}) \mathbf{U}_k \right) \right. \\ & + \left. \left(\mathbf{h}_{k,m,r}^H \mathbf{\Phi} \mathbf{g} \right) \text{Tr} \left(\mathbf{W}_{k,m}^H \mathbf{b}_{k,m}(\bar{\omega}_{m,0}^{RIS}) \mathbf{a}_k^T(\omega_{m,0}^{RIS}) \mathbf{U}_k \right) \right) \\ & + \mu_k \sum_{j=1}^{J_m} \alpha_{k,m,j} \text{Tr} \left(\mathbf{W}_{k,m}^H \mathbf{b}_{k,m}(\bar{\omega}_{m,j}) \mathbf{a}_k^T(\omega_{m,j}) \mathbf{U}_k \right) \\ & + \text{Tr} \left(\mathbf{W}_{k,m}^H \mathbf{Z}_{k,m} \right), \end{aligned} \quad (8)$$

where: $h_{k,m,d} \in \mathbb{C}$ is the response of the direct path from transmitter to the m -th user, $\mathbf{h}_{k,m,r} \in \mathbb{C}^L$ is the response of the path from RIS elements to the m -th user and $\mathbf{g} \in \mathbb{C}^L$ is the response of the path from transmitter to RIS elements. While $(\bar{\omega}_{m,0}, \omega_{m,0})$, $(\bar{\omega}_{m,0}^{RIS}, \omega_{m,0}^{RIS})$, are corresponding angles of arrival and departure for m -th user through direct path, and through RIS, respectively; $\mathbf{b}_{k,m}(\bar{\omega}_{m,0}) \in \mathbb{C}^{N_m}$ is the receive steering vector; $\alpha_{k,m,j} \in \mathbb{C}$ is the response of the j -th undesired path, $(\bar{\omega}_{m,j}, \omega_{m,j})$ are the corresponding angles of arrival and departure, respectively; $\mathbf{W}_{k,m} \in \mathbb{C}^{N_m \times T}$ is the filter employed by the m -th user. $\mathbf{Z}_{k,m} \in \mathbb{C}^{N_m \times T}$ is the disturbance vector.

By taking $\mathbf{w}_{k,m} = \text{vec}(\mathbf{W}_{k,m})$, $\mathbf{B}_{k,m}(\bar{\omega}_{m,j}, \omega_{m,j}) = \mathbf{I}_T \otimes \mathbf{b}_{k,m}(\bar{\omega}_{m,j}) \mathbf{a}_k^T(\omega_{m,j})$ and $\mathbf{z}_{k,m} = \text{vec}(\mathbf{Z}_{k,m})$, the signal can be recast as follows:

$$r_{k,m} = \mu_k f_{k,m} + \mathbf{w}_{k,m}^H \mathbf{z}_{k,m}, \quad (9)$$

where $f_{k,m}$ is the channel response resulting from the superposition of all paths reaching user m on subcarrier k . Notice that $f_{k,m}$ is a complex random variable, and its magnitude follows a Rice distribution whose scale and shape parameters

$$\text{SINR}_k = \frac{\left| h_{k,t,d} \mathbf{w}_k^H \mathbf{B}_k(\varphi_k) \mathbf{u}_k + (\mathbf{h}_{k,t,r}^H \Phi \mathbf{g}) \mathbf{w}_k^H \mathbf{B}_k(\varphi_k^{RIS}) \mathbf{u}_k \right|^2}{\left(\sum_{c=1}^C \sigma_{\eta,k,c}^2 |\mathbf{w}_k^H \mathbf{B}_k(\vartheta_c) \mathbf{u}_k|^2 + \sigma_{z,k}^2 \|\mathbf{w}_k\|^2 \right)}. \quad (5)$$

$$\text{SINR}_k = \frac{\sum_{n=1}^N \left(|h_{k,t,d,n} \mathbf{w}_k^H \mathbf{B}_{k,n}(\varphi_{k,n}) \mathbf{u}_k + (\mathbf{h}_{k,t,r,n}^H \Phi \mathbf{g}_n) \mathbf{w}_k^H \mathbf{B}_{k,n}(\varphi_{k,n}^{RIS}) \mathbf{u}_k|^2 \right)}{\left(\sum_{c=1}^C \sigma_{\eta,k,c}^2 |\mathbf{w}_k^H \mathbf{B}_k(\vartheta_c) \mathbf{u}_k|^2 + \sigma_{z,k}^2 \|\mathbf{w}_k\|^2 \right)}. \quad (6)$$

$$\begin{aligned} \varkappa_{k,m} = & \left| h_{k,m,d} \mathbf{w}_{k,m}^H \mathbf{B}_{k,m}(\bar{\omega}_{m,0}, \omega_{m,0}) \mathbf{u}_k + (\mathbf{h}_{k,m,r}^H \Phi \mathbf{g}) \mathbf{w}_{k,m}^H \mathbf{B}_{k,m}(\bar{\omega}_{m,0}^{RIS}, \omega_{m,0}^{RIS}) \mathbf{u}_k \right|^2 \\ & + \sum_{j=1}^{J_m} \sigma_{\alpha,k,m,j}^2 |\mathbf{w}_{k,m}^H \mathbf{B}_{k,m}(\bar{\omega}_{m,j}, \omega_{m,j}) \mathbf{u}_k|^2. \end{aligned} \quad (10)$$

$$\chi_{k,m} = \frac{\left| h_{k,m,d} \mathbf{w}_{k,m}^H \mathbf{B}_{k,m}(\bar{\omega}_{m,0}, \omega_{m,0}) \mathbf{u}_k + (\mathbf{h}_{k,m,r}^H \Phi \mathbf{g}) \mathbf{w}_{k,m}^H \mathbf{B}_{k,m}(\bar{\omega}_{m,0}^{RIS}, \omega_{m,0}^{RIS}) \mathbf{u}_k \right|^2}{\sum_{j=1}^{J_m} \sigma_{\alpha,k,m,j}^2 |\mathbf{w}_{k,m}^H \mathbf{B}_{k,m}(\bar{\omega}_{m,j}, \omega_{m,j}) \mathbf{u}_k|^2}. \quad (11)$$

can be expressed as (10) and (11), respectively.

The parameter $\varkappa_{k,m} > 0$ is the power received from all paths, while $\chi_{k,m} \geq 0$ provides the ratio of the power along the desired path to that along the undesired paths.

For $MD = 2$, the error probability for the m -th user on the k -th subcarrier can be written as follows [33]:

$$E_{k,m} = \frac{1 + \chi_{k,m}}{2(1 + \chi_{k,m} + \text{SNR}_{k,m})} \exp\left(\frac{-\chi_{k,m} \text{SNR}_{k,m}}{\chi_{k,m} + \text{SNR}_{k,m}}\right), \quad (12)$$

where the signal-to-noise-ratio (SNR) is given by:

$$\text{SNR}_{k,m} = \frac{\varkappa_{k,m}}{\sigma_{z,k,m}^2 \|\mathbf{w}_{k,m}\|^2}. \quad (13)$$

2.3 Transmit Beampattern

The radiated power of the DFRC transmitter towards ζ on subcarrier k can be written as follows [24]:

$$\begin{aligned} \Delta_k(\mathbf{u}_k, \zeta) &= \frac{1}{T} \|\mathbf{a}_k^T(\zeta) \mathbf{u}_k\|^2 \\ &= \frac{1}{T} \mathbf{u}_k^H (\mathbf{I}_T \otimes \mathbf{a}_k^*(\zeta) \mathbf{a}_k^T(\zeta)) \mathbf{u}_k. \end{aligned} \quad (14)$$

Notice that $\Delta_k(\mathbf{u}_k, \zeta) \leq N_t P$ where P is the available power, with equality when all the power is assigned to subcarrier k , i.e., $\mathbf{u}_p = \mathbf{0}_{N_t}$ for $p \neq k$ and $\|\mathbf{u}_k\|^2/T = P$ and $\mathbf{u}_k \propto \mathbf{I}_T \otimes \mathbf{a}_k^*(\zeta)$. It is preferable that the transmit beampattern in each subcarrier illuminate the directions corresponding to the prospective target and the connected users, while reducing the power leakage elsewhere.

3. Problem Formulation

In this section, we formulate the optimization problem of maximizing a radar MI, for a given available power (P),

while maintaining a desired error rate for each user and constraining the transmit beampattern towards specific directions for the system. The conditional mutual information (MI) can be utilized as an appropriate metric for target parameter estimation, while error rate is a performance metric for communication. The design variables are: $\{\mathbf{u}_k\}$ is the transmit code which allocates power across the subcarriers and shapes the transmission beampattern, $\{\mathbf{w}_k, \mathbf{w}_{k,m}\}$ are the receiver filters, which can offer additional degrees of freedom for interference management and $\{\phi\}$ is the phase shift vector of the RIS. Specifically, the problem optimization can be formulated as follows:

$$\begin{aligned} & \max_{\mathbf{u}_k, \mathbf{w}_k, \mathbf{w}_{k,m}, \phi} \text{MI}_k(\mathbf{u}_k, \mathbf{w}_k, \phi) \\ \text{s.t.} & \begin{cases} C1 : \frac{1}{T} \sum_{k=1}^K \|\mathbf{u}_k\|^2 \leq P \\ C2 : \Delta_k(\mathbf{u}_k, \zeta_k) \leq \delta_k N_t P, \forall k \\ C3 : E_{k,m}(\mathbf{u}_k, \mathbf{w}_{k,m}, \phi) \leq \epsilon_{k,m}, \forall k, m, \end{cases} \end{aligned} \quad (15)$$

where $\delta_k \in [0, 1]$. Problem (15) is a complex (non-convex) problem that is difficult to solve analytically.

In problem (15), the first constraint state that the power on the shared subcarriers should be less than or equal to the given power P of the system. The second constraint suggests that the radiated power of the DFRC transmitter towards ζ on subcarrier k should be less than or equal to the value of a predefined radiated power available for each subcarrier. The third constraint state that the error probability for each m -th user on the k -th subcarrier should be less than or equal to a predefined acceptable value of m -th user error rate $\epsilon_{k,m}$.

For the system where the given power is P , we imposed an additional constraint on this system as follows:

$$C4 : \text{SINR}_{k,n}(\mathbf{u}_k, \mathbf{w}_k, \phi) > \text{SINR}_{k,n}^{\min}, \forall k, n, \quad (16)$$

where $C4$ defines the lower limit of $\text{SINR}_{k,n}$ for each target

to satisfy the requirements of the system.

4. Proposed Algorithm

In this section, we explain the algorithm used to solve the optimization problem presented in Sect. 3 based on GA. This algorithm is summarized in Algorithm 1.

4.1 Coding Matrix

For a transmitter with N_t antennas and spanning T symbols, the coding matrix \mathbf{U}_k is a $(N_t \times T)$ matrix. The main objective of this matrix is to transform the original data stream into multiple streams, each intended for transmission via a separate antenna. The signals could be intended for a target, user or could be an RIS.

In this study, the RIS is used in cases where there is no available LoS to the user or target. The RIS will function as a reflector of the signal and also has the additional function of effecting a controlled phase shift of the reflected signal.

For the purpose of the description of the algorithm used in this study, the set of users, targets and RISs are grouped together and the total number of this set is equal to I . The transmit angles toward I items are $\{\zeta_1, \zeta_2, \dots, \zeta_I\}$.

It is important to remember that the system requirements for the user receivers could be based on satisfying a given $\text{SNR}_{k,m}$ or a predefined $\epsilon_{k,m}$. For the radar targets the requirements could be achieving a given set of SINR_k or MI_k etc values. For the system under study, the problem is formulated in Sect. 3. For the determination of the optimal coding matrix \mathbf{U}_k , it is assumed that the coding matrix is a combination of a total of I sub-coding matrices $\{\mathbf{U}_{k,1}, \mathbf{U}_{k,2}, \dots, \mathbf{U}_{k,I}\}$ where the sub-coding matrix $\mathbf{U}_{k,i}$ is the optimal coding matrix required to transmit the signal only to the target, user or RIS. The overall coding matrix, \mathbf{U}_k is related to the sub-coding matrices as follows:

$$\mathbf{U}_k = p_{k,1}\mathbf{U}_{k,1} + p_{k,2}\mathbf{U}_{k,2} + \dots + p_{k,I}\mathbf{U}_{k,I}, \quad (17)$$

where p_i is a factor representing the contribution of sub-coding matrix number i to the total coding matrix. Equation (17) means it is important to determine the set of sub-coding matrices $\{\mathbf{U}_{k,1}, \mathbf{U}_{k,2}, \dots, \mathbf{U}_{k,I}\}$ and to estimate the contribution factors $\{p_{k,1}, p_{k,2}, \dots, p_{k,I}\}$. These factors satisfy the following: $\sum_{i=1}^I p_{k,i} = 1$. Using Eq. (17), we calculate the coding vector \mathbf{u}_k as follows:

$$\mathbf{u}_k = p_{k,1}\mathbf{u}_{k,1} + p_{k,2}\mathbf{u}_{k,2} + \dots + p_{k,I}\mathbf{u}_{k,I}. \quad (18)$$

4.2 User Filter

The filter at any of the M receivers could be calculated using a genetic algorithm approach very similar to that for the coding matrix. It is important to note that the signal is the sum of signals received from different directions as presented in Sect. 2. These directions could correspond to the LoS and that from the RIS and other reflected signals. The genetic

Algorithm 1: Proposed Algorithm for solving problem (23)

```

1 Input  $\varphi_k, \varphi_k^{RIS}, \vartheta_c, \omega_{m,0}, \bar{\omega}_{m,0}, \omega_{m,0}^{RIS}, \bar{\omega}_{m,0}^{RIS}, \omega_{m,j},$ 
 $\bar{\omega}_{m,j}, \delta_k, \epsilon_{k,m}$ , maximum iterations
2 Initialize: elements of
 $\{\mathbf{u}_{k,i}\}, \{\mathbf{w}_{k,n}\}, \{\mathbf{w}_{k,m,j}\}, \{p_{k,i}\}, \{p_{k,rad,n}\}, \{p_{k,m,j}\}, \phi$ 
with random values ;
3 for each of  $i = 1, 2, \dots, I$  users/targets/RIS do
4   Repeat
5     Calculate  $\Delta(\mathbf{u}_{k,i}, \zeta_i)$  according to (14)
6     Repeat for each element of  $\mathbf{u}_{k,i}$  do
7       Calculate  $\Delta(\mathbf{u}_{k,i}, \zeta_i)$ 
8       Update  $\mathbf{u}_{k,i}$  using bisection method
9       Update  $\phi$ 
10    Until no further changes in  $\Delta(\mathbf{u}_{k,i}, \zeta_i)$ 
11  end
12  Until no further changes in  $\Delta(\mathbf{u}_{k,i}, \zeta_i)$ 
13 end
14 Repeat for each  $m$ -th user , for each  $j = \text{LoS}$  and RIS do
15   Repeat for each element of  $\mathbf{w}_{k,m,j}$  do
16     Calculate user receive beampattern as mentioned in
section (5.2)
17     Update  $\mathbf{w}_{k,m,j}$  using bisection method
18     Update  $\phi$ 
19   end
20   Until no further changes in user receive beampattern
21 end
22 Until no further changes in user receive beampattern
23 for each of  $n = 1, 2, \dots$  (targets/RIS) do
24   Repeat
25     Repeat for each element of  $\mathbf{w}_{k,n}$  do
26       Calculate radar receive beampattern as mentioned
in section (5.2)
27       Update  $\mathbf{w}_{k,n}$  using bisection method
28       Update  $\phi$ 
29     Until no further changes in radar receive beampattern
30   end
31   Until no further changes in radar receive beampattern
32 end
33 Repeat
34   for each user identifier  $m$  do
35     Calculate  $E_{k,m}$ 
36     Calculate  $p_{k,m}$  according to (24)
37     If C1, C2 and C3 are satisfied , then
38     Update  $p_{k,m}$  and  $\mathbf{u}_k$  according to (18)
39     for each  $j = \text{LoS}$  and RIS do
40       Update  $p_{k,m,j}$  according to section (4.7)
41       Update  $\mathbf{w}_{k,m}$  and  $\phi$  according to (20) and section
(4.6)
42     end
43   end
44   for each target and RIS identifier  $n$  do
45     Calculate new  $p_{k,n}$  according to section (4.1)
46     If all constrains are satisfied , then
47       update  $p_{k,n}$  ,  $\mathbf{u}_k$  and  $\phi$ 
48     Calculate new  $p_{k,rad,n}$  according to section (4.7)
49     If all constrains are satisfied, then
50       update  $p_{k,rad,n}$ 
51       update  $\mathbf{w}_k$  according to (22)
52     Calculate  $\text{MI}_k$  according to (7)
53     If  $\text{MI}_k$  is grater than  $\text{MI}_k^{max}$  , then
54       Update  $p_{k,rad,n}$  ,  $\mathbf{w}_k$  ,  $\phi$  and  $\text{MI}_k^{max}$ 
55   end
56 Until no further changes in  $\text{MI}_k$  or maximum iterations reached

```

optimization approach takes this into account. In the same way, as for the coding matrix, the total filter employed at a receiver, $\mathbf{W}_{k,m}$, can be represented as follows:

$$\mathbf{W}_{k,m} = p_{k,m,1}\mathbf{W}_{k,m,1} + p_{k,m,2}\mathbf{W}_{k,m,2} + \cdots \quad (19)$$

From the above Eq. (19), we calculate the user filter vector $\mathbf{w}_{k,m}$ as follows:

$$\mathbf{w}_{k,m} = p_{k,m,1}\mathbf{w}_{k,m,1} + p_{k,m,2}\mathbf{w}_{k,m,2} + \cdots, \quad (20)$$

where $\mathbf{w}_{k,m,1}, \mathbf{w}_{k,m,2}, \cdots$ etc are the user sub-filters.

4.3 Radar Filter

The radar expects to receive signals reflected from the LoS targets and also via the RIS if applicable. Therefore, the total filter employed at a radar receiver, \mathbf{W}_k , can be represented as follows:

$$\mathbf{W}_k = p_{k,rad,1}\mathbf{W}_{k,1} + p_{k,rad,2}\mathbf{W}_{k,2} + \cdots \quad (21)$$

From the above Eq. (21), we calculate the radar filter vector \mathbf{w}_k as follows:

$$\mathbf{w}_k = p_{k,rad,1}\mathbf{w}_{k,1} + p_{k,rad,2}\mathbf{w}_{k,2} + \cdots, \quad (22)$$

where $\mathbf{w}_{k,1}, \mathbf{w}_{k,2}, \cdots$ etc are the radar sub-filters.

According to Eqs. (18), (20) and (22), we redefine the original optimization problem in (15) as follows:

$$\max_{\Gamma} \text{MI}_k(\mathbf{u}_k, \mathbf{w}_k, \boldsymbol{\phi}), \quad (23)$$

where $\Gamma = \{\mathbf{u}_{k,i}, \{\mathbf{w}_{k,n}\}, \{\mathbf{w}_{k,m,j}\}, \{p_{k,i}\}, \{p_{k,rad,n}\}, \{p_{k,m,j}\}, \boldsymbol{\phi}$ while satisfying the all constraints defined in (15) and (16).

4.4 Sub-Coding Vectors

The Genetic Algorithm (GA) is a potent evolutionary algorithm variant that can tackle non-convex optimization problems [34]. This study uses the GA to determine the sub-coding vectors to solve the multi-objective problem defined in (23).

The algorithm described here is applicable for uniform and non-uniform linear arrays. The fitness function used to determine the sub-coding vectors is the value of the power $\Delta(\mathbf{u}_{k,i}, \zeta_i)$ in (14) in the direction of the given user, target or RIS. The amplitude of $\mathbf{u}_{k,i}$ is taken to be equal to unity and therefore the optimization space will be over the phase range $[0, 2\pi]$. The algorithm starts by a set of random values for $\mathbf{u}_{k,i}$ and the value of $\Delta(\mathbf{u}_{k,i}, \zeta_i)$ is computed.

The search process used in this paper implements an initial increment of $\Delta\zeta_i = \pi/2$. The value of ζ_i is changed by $+\Delta\zeta_i$ and $-\Delta\zeta_i$ to determine the direction of the next candidate. The outcome of this initial search is to determine the low and high values of ζ_i for the interval where the maximum of the power $\Delta(\mathbf{u}_{k,i}, \zeta_i)$ is located, then we implement the standard bisection method where the value of $\Delta\zeta_i$

is halved in each step. A minimum value $\Delta\zeta_i = 1^\circ$ is used in this study. The maximum number of iterations for this process to equal to 7 iterations.

The above process is repeated for all elements until no further change is detected. By the end of this process a set of I sub-coding vectors $\{\mathbf{u}_{k,1}, \mathbf{u}_{k,2}, \cdots, \mathbf{u}_{k,I}\}$ are determined.

4.5 Sub-Filter Vectors

In this study the user receives a signal from two possible directions; viz. the LoS path and the RIS path. We then define the sub-filter vectors for the m -th user as $\mathbf{w}_{k,m,1}$ and $\mathbf{w}_{k,m,2}$ for the two paths. The determination of the user sub-filter vectors follows a procedure that is similar to that of the sub-coding vectors in Sect. 4.4.

The radar sub-filter vectors correspond to the LoS path to the targets and RIS is applicable; also the determination of the radar sub-filter vectors follows the procedure that is similar to that of sub-coding vectors in Sect. 4.4.

4.6 RIS Phase Shift

With reference to (8) and for optimum performance, the two components (the LoS and via the RIS) should be in phase at the m -th user.

Let us assume the phase angle of the LoS component in (8) is (θ_{LoS}) . Also, we assume no phase shift due to the RIS and the total phase angle due to the RIS component (θ_{RIS}) , where the RIS functions as a reflector only and it introduces no phase shift. To achieve an optimum signal, the designated RIS element should introduce a phase shift $\theta_l = \theta_{LoS} - \theta_{RIS}$. The same procedure is applicable to the RIS phase shift with regards to the signal received at the radar for the targets given in (3).

The phase shift vector, $\boldsymbol{\phi}$, of the RIS is optimized at each step to achieve an optimum solution.

4.7 System Optimization

The solution of the multi-objective problem defined in (23) requires consideration of the effects of the contribution factors on the system performance.

The first stage of the algorithm is to determine the set of sub-coding vectors $\{\mathbf{u}_{k,1}, \mathbf{u}_{k,2}, \cdots, \mathbf{u}_{k,I}\}$, the set of user sub-filters $\{\mathbf{w}_{k,m,1}, \mathbf{w}_{k,m,2}, \cdots\}$ and the set of radar sub-filters as $\{\mathbf{w}_{k,1}, \mathbf{w}_{k,2}, \cdots\}$, this is described in Sect. 4.4 and Sect. 4.5.

The next stage is to estimate the contribution factors $p_{k,1}, p_{k,2}, \cdots, p_{k,I}$ in (18), $p_{k,m,1}, p_{k,m,2}, \cdots$, etc in (20) and $p_{k,rad,1}, p_{k,rad,2}, \cdots$, etc in (22).

The algorithm starts by selecting a random set of contribution factors for the LoS entities served by the transmitter. Also, the algorithm selects a random set of contribution factors in Eqs. (18), (20) and (22).

The error probability $E_{k,m}$ for each m -th user is computed using Eq. (12). For the purpose of the algorithm, we define an error probability for each m -th user $\epsilon'_{k,m}$ where $\epsilon'_{k,m}$ is less than $\epsilon_{k,m}$. The range $[\epsilon'_{k,m} - \epsilon_{k,m}]$ is considered to be

an acceptable range for the algorithm. If the calculated $E_{k,m}$ at m -th user is too high ($E_{k,m} > \epsilon_{k,m}$), then the contribution factor $p_{k,m}$, for the direction of the m -th user is increased, this will increase the power in this direction. Also, if the calculated $E_{k,m}$ at the m -th user is too low ($E_{k,m} < \epsilon'_{k,m}$), then the contribution factor for the direction is reduced and this will reduce the power in this direction.

To improve the performance of this process, we employ a dynamic increment $\Delta p_{k,m}$ where $\Delta p_{k,m}$ is computed as a function of the calculated $E_{k,m}$. The function implemented in this study is given by:

$$\Delta p_{k,m} \propto \log(E_{k,m}/\epsilon_{k,m}). \quad (24)$$

Changes in the transmit contribution factors dictate updates in the user and radar filters. For the user filter, we also implement a GA to optimize the resulting $E_{k,m}$. The filter contribution factors are updated using dynamic increments $\Delta p_{k,m,j}$.

The objective of the updates applied to the user filter is to achieve the minimum possible error probability. The increments, $\Delta p_{k,m,j}$, used to update the user filter follow a bisection method where an initial increment of $\Delta p_{k,m,j} = 0.1$ and the minimum value of 0.01 is imposed. This algorithm is applied only when the specific user receives a signal from more than one path. If the user receives from one path, then only the contribution of that path is always applied. The radar receives signals from the LoS targets and RIS if applicable. The radar filter should be modified to optimize MI_k . Our algorithm updates the contribution factors successively searching for the maximum MI_k . The increments follow a bisection method as described for the user filter.

The phase shift vector, ϕ , of the RIS is updated at each step to achieve an optimum solution as described in Sect. 4.6.

5. Simulation Results and Performance Analysis

5.1 System Set-Up

An OFDM RIS-Assisted MIMO DFRC system with a maximum power of $P = 20$ dBW on shared subcarriers is considered. The center frequency of the k -th subcarrier is defined as $\nu_k = \nu_0 + (k - 1)\Delta\nu$, where $\nu_0 = 2$ GHz and $\Delta\nu = 100$ kHz. The transmitter is a uniform array of antenna and each array has a uniform element spacing of $c/(2\max(\nu_k))$.

In the radar model, we inspect a randomly selected different direction within the range of $[-60^\circ, 60^\circ]$ on each subcarrier. We set $\sigma_{z,k}^2 = -150.0$ dBW, and the clutter directions are randomly chosen in $[-60^\circ, 60^\circ]$, while $\sigma_{\eta,k,c}^2$ for each clutter element is assumed to be -150.0 dBW. The distance between each target and the DFRC transceiver is chosen in the range of $[7 - 10$ km].

For the communication model, the corresponding angles of arrival and departure are sampled from a uniform distribution within $[-60^\circ, 60^\circ]$ and we set $\sigma_{z,k,m}^2 = -145.0$ dBW. The distance between each user and the DFRC transceiver is chosen in the range of $[1.3 - 1.8$ km].

Additional parameters are number of transmit antennas $N_t = 15$, number of receive antennas $N_r = 8$, number of user receive antennas $N_c = 4$, number of subcarrier $k = 4$ and constellation size $MD = 2$.

5.2 Analysis of MIMO OFDM DFRC System Performance with and without RIS Assistance

In this study, we examine a MIMO OFDM DFRC system with the assistance of a RIS, which considers two targets and three users. We define the transmit beampattern for one subcarrier as per Eq. (14). Also, the radar and user receive beampatterns are defined as $\|\mathbf{W}_k^H \mathbf{b}_k(\zeta)\|^2/T$ and $\|\mathbf{W}_{k,m}^H \mathbf{b}_{k,m}(\zeta)\|^2/T$, respectively. In this instance, we set $\epsilon_{k,m} = 10^{-6}$, $\delta_k = 0.02$ and $\text{SINR}_{k,n}^{\min} = 3$ dB.

First, the proposed algorithm was compared with the semidefinite relaxation (SDR) method [25] and the alternating direction method of multipliers (ADMM) [35] for a simple scenario of one target and one user as shown in Fig. 2. The SDR algorithm is a widely used optimization technique for solving the non-convex problem, it serves as a benchmark algorithm in many radar-communication studies. Also, the ADMM algorithm can solve the non-convex problem, iteratively. The figure depicts the optimized transmit beampattern on one subcarrier (red, solid) using GA, (blue, solid) using SDR and (cyan, solid) using ADMM. The vertical lines demonstrate the locations of a target at -30° (black, solid), a user at 40° (green, solid), as well as the positions of the clutter (red, dashed). The performance of the ADMM algorithm was low compared with GA and SDR algorithms. The maximum error between the GA and SDR beampatterns is found to be around 6%. The efficiency of the proposed GA algorithm as measured by execution time is found to be better than SDR algorithm by 10% for this scenario.

The first scenario considers a MIMO OFDM DFRC system without RIS. Fig. 3 presents the calculation of MI_k at the radar receiver against the contribution factor of sub-

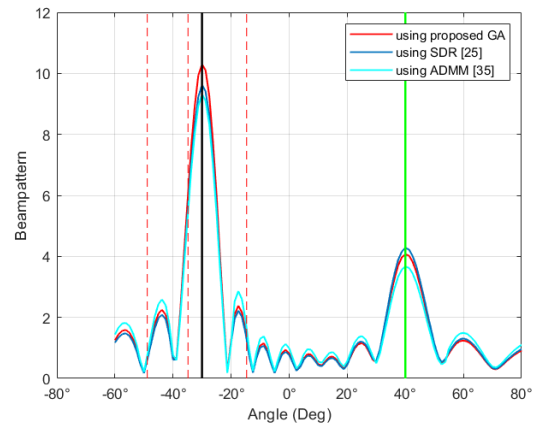


Fig. 2 Transmit beampattern (unitless) (red, solid) using GA, (blue, solid) using SDR, (cyan, solid) using ADMM, on one subcarrier, along with one target (black, solid) with the presence of the clutter (red, dashed) and one user (green, solid).

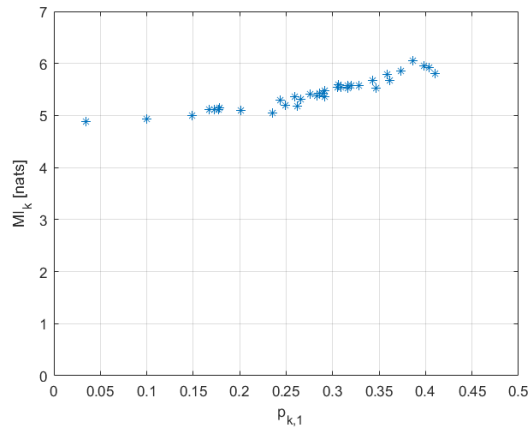
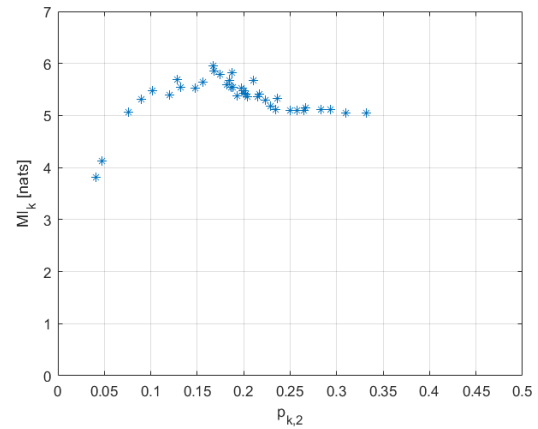
((a)) MI_k versus $p_{k,1}$.((b)) MI_k versus $p_{k,2}$.

Fig. 3 MI_k versus the contribution factor of sub-coding vectors towards target 1 and 2 in transmit coding vector for the case when no RIS is used. MI_k versus $p_{k,1}$ in (a) MI_k versus $p_{k,2}$ in (b).

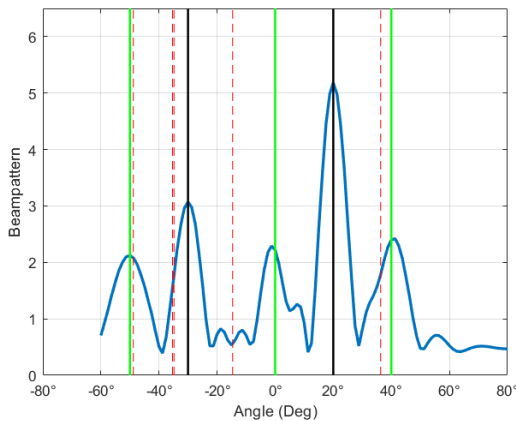


Fig. 4 Transmit beampattern (unitless) (blue, solid), on one subcarrier, along with two targets (black, solid) with the presence of the clutter (red, dashed) and three users (green, solid), in the case of without RIS.

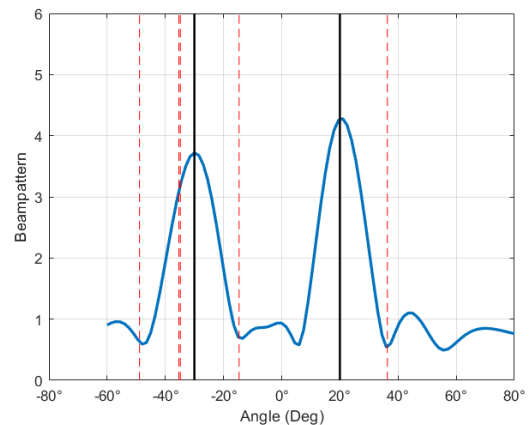


Fig. 5 Radar receive beampattern (unitless) (blue, solid), on one subcarrier, along with two targets (black, solid) and clutter (red, dashed), in the case of without RIS.

coding vectors towards target 1 and 2 in transmit coding vector $p_{k,1}$ and $p_{k,2}$ in the direction of target 1 (considered at 20°) and target 2 (considered at -30°). The scatter points are obtained for different runs as described in Algorithm 1.

We note that the optimum value of MI_k is achieved as the combination of $p_{k,1} = 0.38$ and $p_{k,2} = 0.155$. This figure indicates that for values of $p_{k,1}$ greater than 0.41, the error rate constraint, C3, will no longer be satisfied. This is also applicable for $p_{k,2}$ greater than 0.33.

The study of the relationship between $SINR_{k,1}$ and $SINR_{k,2}$ against $p_{k,1}$ and $p_{k,2}$ manifests a peak value for both $SINR_{k,1}$ and $SINR_{k,2}$ at the common point $p_{k,1} = 0.38$ and $p_{k,2} = 0.155$.

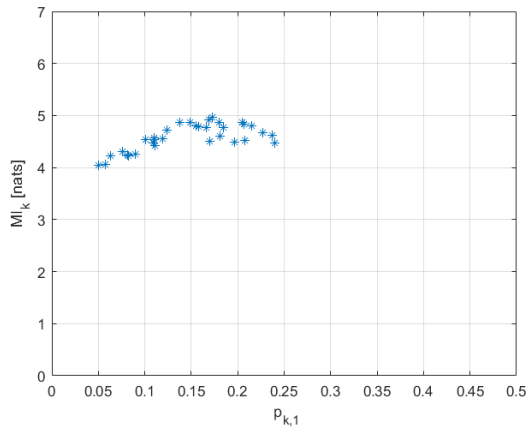
Figure 4 depicts the optimized transmit beampattern (blue, solid), on one subcarrier. The vertical lines demonstrate the locations of two targets at -30° and 20° , three users at -50° , 0° , and 20° , as well as the positions of the clutter. It is noticeable from the examination that the transmit beampattern peaks at the target locations. Further, Fig. 5 illustrates the radar receive beampatterns on one subcarrier

(blue, solid) along with two targets and the clutter. Consistent with the transmit beampattern, the radar receive beampattern also peaks at the target locations.

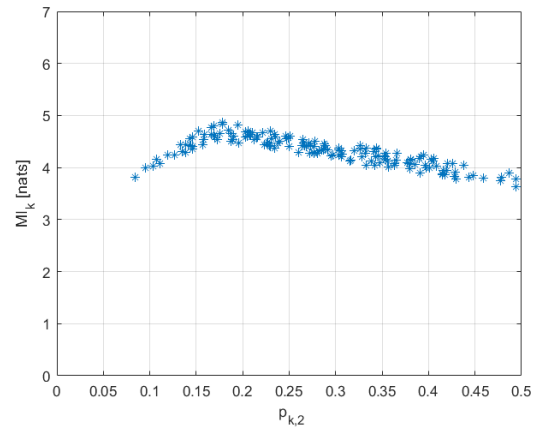
The second scenario involves a MIMO OFDM DFRC system with the assistance of a RIS panel at 60° . In this instance, the user positioned at 40° is considered to be in a blind spot. As a result, there is no LoS beam, and the user receives only the beam reflected from the RIS panel. Also, we consider target 1, located at 20° , receives both LoS beam, as well as reflection beam from the RIS panel.

Figure 6 presents the MI_k versus the contribution factor of sub-coding vectors towards target 1 and 2 in transmit coding vector $p_{k,1}$ in (a), $p_{k,2}$ and the contribution factor in (b). The optimal value of MI_k is achieved at common point $p_{k,1} = 0.151$ and $p_{k,2} = 0.17$. Similarly, $SINR_{k,1}$ and $SINR_{k,2}$ have peak values at the same $p_{k,1}$ and $p_{k,2}$ values above.

Figure 7 shows the optimized transmit beampattern (blue, solid), the vertical lines indicate the locations of the two targets and three users, the locations of the clutter, and



((a)) MI_k versus $p_{k,1}$.



((b)) MI_k versus $p_{k,2}$.

Fig. 6 MI_k versus the contribution factor of sub-coding vectors towards target 1 and 2 in transmit coding vector in the case of with RIS. MI_k versus $p_{k,1}$ in (a) MI_k versus $p_{k,2}$ in (b).

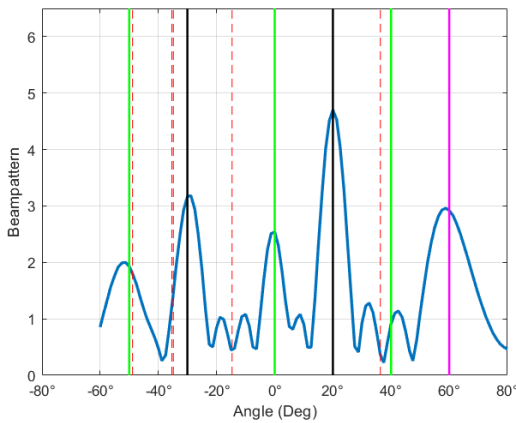


Fig. 7 Transmit beampattern (unitless) (blue, solid), on one subcarrier, along with two targets (black, solid) with the presence of the clutter (red, dashed) and three users (green, solid), in the case of RIS panel (Magenta, solid).

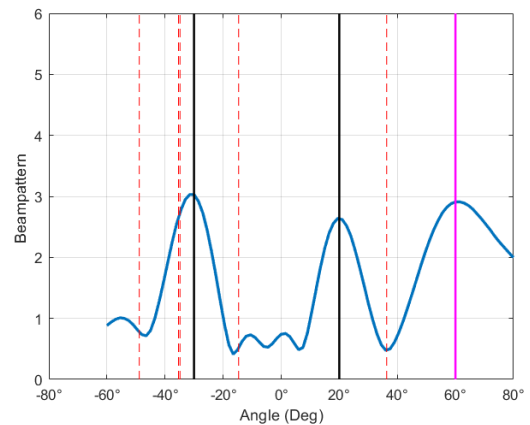


Fig. 8 Radar receive beampattern (unitless) (blue, solid), on one subcarrier, along with two targets (black, solid) and clutter (red, dashed), in the case of RIS panel (Magenta, solid).

the RIS panel (Magenta, solid) at 60° . It is obvious that the user at 40° has no LoS direction, therefore it receives the only beam reflection from the RIS panel. In accordance with the same scenario, Fig. 8 shows the radar receive beampattern (blue, solid), on one subcarrier, along with two targets and clutter, and RIS panel. The radar receive beampattern peaks at the targets locations, with an additional peak for target 1 due to the RIS panel. For the radar, target 1, the signal at the radar receiver has two components, the direct LoS and via the RIS. For the scenario at hand, the power received via the RIS is found to be 50–70% of the direct LoS; the ratio depends on the contribution factors.

The third scenario is similar to scenario 2, the only difference is that target 1 receives only the LoS beam, while in scenario 2, target 1 receives both the LoS beam and reflected beam from RIS. The value of MI_k for this scenario shown together with MI_k of scenario 2, which is presented in Fig. 9. To demonstrate the effect of the RIS on the performance, we calculated MI_k with and without RIS, and it is found that the

presence of RIS improves MI_k by about 12%.

In a different scenario not detailed here, the user at -50° receives both a LoS beam and a reflection beam from the RIS panel. In this situation, the power received via the RIS is found to be 25% of the direct LoS power.

The MI_k for all four subcarriers was calculated and found to be closely aligned, falling within the range of 5–7 nats. Similarly, the $SINR_{k,1}$ for target 1 and $SINR_{k,2}$ for target 2 were observed to fall within the range of 14–15 dB.

Figure 10 shows the MI_k versus $\epsilon_{k,m}$ for scenario 2 and scenario 3, where $\epsilon_{k,m}$ was varied in the range $10^{-7} - 10^{-4}$. At a lower value of $\epsilon_{k,m}$ more power should be transmitted towards the users at the expense of the power towards targets. This will result in lower MI_k . The beam reflected from the RIS towards the target improves the MI_k by about 12%. The primary objective of the RIS in this scenario is to satisfy the communication objective for the user at 40° where there is no LoS path, however the RIS enhances the radar performance in this scenario. The maximum number of iterations required for our proposed algorithm to converge is about 30 iterations

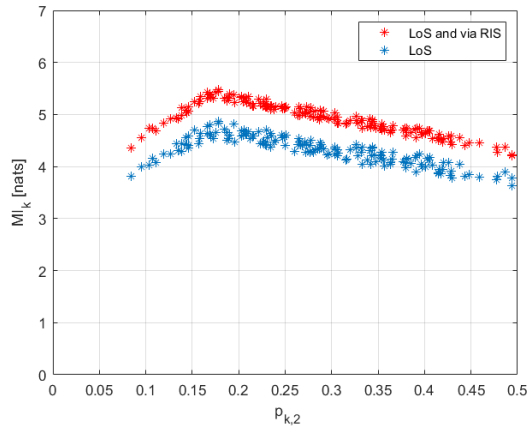


Fig. 9 MI_k versus the contribution factor the contribution factor of sub-coding vector towards target 2 in transmit coding vector $p_{k,2}$, in the case of target 2 receives LoS beam only while target 1 receives the LoS beam only or both the LoS beam together with beam via RIS.

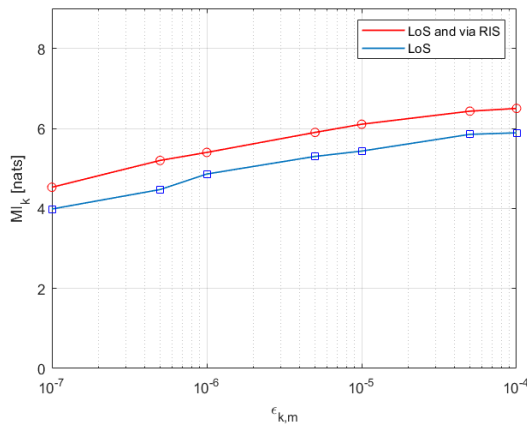


Fig. 10 MI_k versus $\epsilon_{k,m}$: target 1 receives the LoS beam only or both the LoS beam together with beam via RIS.

for the scenarios discussed in this study.

6. Conclusion

In this paper, we considered a MIMO OFDM DFRC system with the assistance of RIS. The transmit waveforms and the receive filters have been designed to maximize radar performance according to MI optimization for multi-targets while constraining the user error rate and beampattern towards specific directions on average radiated power. The system design results in a non-convex problem, which has been optimally solved computationally via a GA. The performance of the GA was improved by the use of bisection method together with the dynamic update of the coding matrix. The numerical results showed that the RIS significantly improves the MIMO OFDM DFRC system, particularly in areas where there are blind spots or blocks.

There may be future developments where multiple RISs can be configured to create constructive interference, nullify destructive interference, and improve signal quality, which can result in better communication performance and radar

detection. In addition, by deploying multiple RIS panels, the DFRC system may gain a greater degree of flexibility in resource allocation.

Acknowledgments

The authors would like to express their sincere gratitude to Prof. Sharief F. Babiker for fruitful discussions and Dr. Smahi Abl for shaping and refining this work.

References

- [1] H. Griffiths, L. Cohen, S. Watts, E. Mokole, C. Baker, M. Wicks, and S. Blunt, "Radar spectrum engineering and management: Technical and regulatory issues," *Proc. IEEE*, vol.103, no.1, pp.85–102, Jan. 2015.
- [2] B. Paul, A.R. Chiriyath, and D.W. Bliss, "Survey of RF communications and sensing convergence research," *IEEE Access*, vol.5, pp.252–270, 2017.
- [3] A. Martone and M. Amin, "A view on radar and communication systems coexistence and dual functionality in the era of spectrum sensing," *Digital Signal Processing*, vol.119, p.103135, Dec. 2021.
- [4] F. Liu, C. Masouros, A.P. Petropulu, H. Griffiths, and L. Hanzo, "Joint radar and communication design: Applications, state-of-the-art, and the road ahead," *IEEE Trans. Commun.*, vol.68, no.6, pp.3834–3862, June 2020.
- [5] C.G. Tsinos, A. Arora, S. Chatzinotas, and B. Ottersten, "Joint transmit waveform and receive filter design for dual-function radar-communication systems," *IEEE J. Sel. Topics Signal Process.*, vol.15, no.6, pp.1378–1392, Nov. 2021.
- [6] C. Shi, F. Wang, S. Salous, and J. Zhou, "Low probability of intercept-based optimal OFDM waveform design strategy for an integrated radar and communications system," *IEEE Access*, vol.6, pp.57689–57699, 2018.
- [7] E. Uhlemann, "Time for autonomous vehicles to connect [connected vehicles]," *IEEE Veh. Technol. Mag.*, vol.13, no.3, pp.10–13, Sept. 2018.
- [8] F. Liu and C. Masouros, "A tutorial on joint radar and communication transmission for vehicular networks — Part I: Background and fundamentals," *IEEE Commun. Lett.*, vol.25, no.2, pp.322–326, 2021.
- [9] M. Ashraf, B. Tan, D. Moltchanov, J.S. Thompson, and M. Valkama, "Joint optimization of radar and communications performance in 6G cellular systems," *IEEE Trans. Green Commun. Netw.*, vol.7, no.1, pp.522–536, 2023.
- [10] N.A.A. Elhag, P. Wei, X. Tang, M. Mohammad, and A. Smahi, "Optimal power allocation strategy for a MIMO-integrated radar and communication system based OFDM waveform," *2022 3rd Information Communication Technologies Conference (ICTC)*, pp.91–96, May 2022.
- [11] D. Ma, N. Shlezinger, T. Huang, Y. Liu, and Y.C. Eldar, "Joint radar-communication strategies for autonomous vehicles: Combining two key automotive technologies," *IEEE Signal Process. Mag.*, vol.37, no.4, pp.85–97, June 2020.
- [12] S. Buzzi, E. Grossi, M. Lops, and L. Venturino, "Foundations of MIMO radar detection aided by reconfigurable intelligent surfaces," *IEEE Trans. Signal Process.*, vol.70, pp.1749–1763, 2022.
- [13] C. Pan, H. Ren, K. Wang, J.F. Kolb, M. Elkhshlan, M. Chen, M.D. Renzo, Y. Hao, J. Wang, A.L. Swindlehurst, X. You, and L. Hanzo, "Reconfigurable intelligent surfaces for 6G systems: Principles, applications, and research directions," *IEEE Commun. Mag.*, vol.59, no.6, pp.14–20, June 2021.
- [14] M.A. ElMossallamy, H. Zhang, L. Song, K.G. Seddik, Z. Han, and G.Y. Li, "Reconfigurable intelligent surfaces for wireless communications: Principles, challenges, and opportunities," *IEEE Trans.*

- Cogn. Commun. Netw., vol.6, no.3, pp.990–1002, Sept. 2020.
- [15] Q. Wu and R. Zhang, "Towards smart and reconfigurable environment: Intelligent reflecting surface aided wireless network," *IEEE Commun. Mag.*, vol.58, no.1, pp.106–112, Jan. 2020.
- [16] S. Abeywickrama, R. Zhang, Q. Wu, and C. Yuen, "Intelligent reflecting surface: Practical phase shift model and beamforming optimization," *IEEE Trans. Commun.*, vol.68, no.9, pp.5849–5863, Sept. 2020.
- [17] Q. Wu and R. Zhang, "Intelligent reflecting surface enhanced wireless network via joint active and passive beamforming," *IEEE Trans. Wireless Commun.*, vol.18, no.11, pp.5394–5409, Nov. 2019.
- [18] C. Liaskos, A. Tsioliaridou, A. Pitsillides, S. Ioannidis, and I. Akyildiz, "Using any surface to realize a new paradigm for wireless communications," *Commun. ACM*, vol.61, no.11, pp.30–33, Oct. 2018.
- [19] S.V. Hum and J. Perruisseau-Carrier, "Reconfigurable reflectarrays and array lenses for dynamic antenna beam control: A review," *IEEE Trans. Antennas Propag.*, vol.62, no.1, pp.183–198, Jan. 2014.
- [20] C. Shi, F. Wang, M. Sellathurai, J. Zhou, and S. Salous, "Low probability of intercept-based optimal power allocation scheme for an integrated multistatic radar and communication system," *IEEE Syst. J.*, vol.14, no.1, pp.983–994, March 2020.
- [21] A. Ahmed, Y.D. Zhang, and B. Himed, "Distributed dual-function radar-communication MIMO system with optimized resource allocation," 2019 IEEE Radar Conference (RadarConf), pp.1–5, April 2019.
- [22] C. Shi, Y. Wang, F. Wang, S. Salous, and J. Zhou, "Power resource allocation scheme for distributed MIMO dual-function radar-communication system based on low probability of intercept," *Digital Signal Processing*, vol.106, p.102850, Nov. 2020.
- [23] Z. Xu and A. Petropulu, "A bandwidth efficient dual-function radar communication system based on a MIMO radar using OFDM waveforms," *IEEE Trans. Signal Process.*, vol.71, pp.401–416, 2023.
- [24] J. Johnston, L. Venturino, E. Grossi, M. Lops, and X. Wang, "MIMO OFDM dual-function radar-communication under error rate and beampattern constraints," *IEEE J. Sel. Areas Commun.*, vol.40, no.6, pp.1951–1964, June 2022.
- [25] G. Zhang, C. Shen, F. Liu, Y. Lin, and Z. Zhong, "Beampattern design for RIS-aided dual-functional radar and communication systems," *GLOBECOM 2022 - 2022 IEEE Global Communications Conference*, pp.3899–3904, Dec. 2022.
- [26] S. Yan, S. Cai, W. Xia, J. Zhang, and S. Xia, "A reconfigurable intelligent surface aided dual-function radar and communication system," 2022 2nd IEEE International Symposium on Joint Communications & Sensing (JC&S), pp.1–6, March 2022.
- [27] W. Zhong, Z. Yu, Y. Wu, F. Zhou, Q. Wu, and N. Al-Dhahir, "Resource allocation for an IRS-assisted dual-functional radar and communication system: Energy efficiency maximization," *IEEE Trans. Green Commun. Netw.*, vol.7, no.1, pp.469–482, March 2023.
- [28] G. Gradoni and M.D. Renzo, "End-to-end mutual coupling aware communication model for reconfigurable intelligent surfaces: An electromagnetic-compliant approach based on mutual impedances," *IEEE Wireless Commun. Lett.*, vol.10, no.5, pp.938–942, May 2021.
- [29] S.W. Ellingson, "Path loss in reconfigurable intelligent surface-enabled channels," 2021 IEEE 32nd Annual International Symposium on Personal, Indoor and Mobile Radio Communications (PIMRC), pp.829–835, Sept. 2021.
- [30] W. Tang, M.Z. Chen, X. Chen, J.Y. Dai, Y. Han, M.D. Renzo, Y. Zeng, S. Jin, Q. Cheng, and T.J. Cui, "Wireless communications with reconfigurable intelligent surface: Path loss modeling and experimental measurement," *IEEE Trans. Wireless Commun.*, vol.20, no.1, pp.421–439, Jan. 2021.
- [31] F.H. Danufane, M.D. Renzo, J. de Rosny, and S. Tretyakov, "On the path-loss of reconfigurable intelligent surfaces: An approach based on Green's theorem applied to vector fields," *IEEE Trans. Commun.*, vol.69, no.8, pp.5573–5592, Aug. 2021.
- [32] J.C.B. Garcia, A. Sibille, and M. Kamoun, "Reconfigurable intelligent surfaces: Bridging the gap between scattering and reflection," *IEEE J. Sel. Areas Commun.*, vol.38, no.11, pp.2538–2547, Nov. 2020.
- [33] J. Roberts and J. Bargallo, "Dpsk performance for indoor wireless Rician fading channels," *IEEE Trans. Commun.*, vol.42, no.2/3/4, pp.592–596, Feb. 1994.
- [34] F. Wang, G. Xu, and M. Wang, "An improved genetic algorithm for constrained optimization problems," *IEEE Access*, vol.11, pp.10032–10044, 2023.
- [35] A. Saleem, A. Basit, M.F. Munir, A. Waseem, W. Khan, A.N. Malik, S.A. AlQahtani, A. Daraz, and P. Pathak, "Alternating direction method of multipliers-based constant modulus waveform design for dual-function radar-communication systems," *Entropy*, vol.25, no.7, p.1027, June 2023.



Nihad A. A. Elhag received a B.Sc. in electronic engineering and an M.Sc. in communication engineering, from the University of Gezira, Sudan. She is currently working toward the Ph.D. degree in the School of Information and Communication Engineering, University of Electronic Science and Technology of China, Chengdu, China. Her research interests are waveform design for integrated MIMO radar and communication systems and optimization.



Liang Liu received the B.S. and Ph.D. degrees in information and communication engineering from the University of Electronic Science and Technology of China, Chengdu, China, in 2012 and 2018, respectively. From 2018 to 2020, he was an Engineer with the Southwest China Institute of Electronic Technology, Chengdu. He is currently an Assistant Researcher with the School of Information and Communication Engineering, University of Electronic Science and Technology of China.

His research interests include sampling theory, array signal processing.



Ping Wei received B.S. and M.S. degrees both in the electronic engineering from Beijing Institute of Technology in 1986 and 1989, respectively. He received his Ph.D. degree in communication and electronic system from the University of Electronic Science and Technology of China in 1996. He is now a professor in the School of Information and Communication Engineering of UESTC. His research interests include spectral analysis, array signal processing, electronic surveillance, and communication

signal processing.



Hongshu Liao was born in 1978. She is an associate professor of University of Electronic Science and Technology of China. Her research interests include communication signal analysis and channel code identification. She has published many papers in IET communication, Journal on Communications and other conferences, and obtained more than 10 authorized patents.



Lin Gao received the B.S., M.S. and Ph.D. degrees all in information and communication engineering from the University of Electronic Science and Technology of China. From 2018 to 2020, he was a postdoc research fellow at the Department of Information Engineering of the University of Florence. Currently he is a Lecturer with the School of Information and Communication Engineering, University of Electronic Science and Technology of China. His research interests include statistical signal processing, target localization, multi-sensor multi-target tracking, information fusion and multi-vehicle SLAM.